Chinese Journal of Aeronautics, (2014),27(4): 772–780

Chinese Society of Aeronautics and Astronautics
& Beihang University

Chinese Journal of Aeronautics

cja@buaa.edu.cn
www.sciencedirect.com

Low-frequency unsteadiness of vortex wakes over slender bodies at high angle of attack

Ma Baofeng *, **Huang Yu**, **Liu Tongxin**

Ministry-of-Education Key Laboratory of Fluid Mechanics, Beihang University, Beijing 100191, China

Received 5 August 2013; revised 18 March 2014; accepted 25 March 2014
Available online 4 July 2014

KEYWORDS

Aerodynamics;
Experiments;
Fluid dynamics;
Unsteady flow;
Vortex flow

Abstract A type of flow unsteadiness with low frequencies and large amplitude was investigated experimentally for vortex wakes around an ogive-tangent cylinder. The experiments were carried out at angles of attack of 60–80° and subcritical Reynolds numbers of $0.6–1.8 \times 10^5$. The reduced frequencies of the unsteadiness are between 0.038 and 0.072, much less than the frequency of Karman vortex shedding. The unsteady flow induces large fluctuations of sectional side forces. The results of pressure measurements and particle image velocimetry indicate that the flow unsteadiness comes from periodic oscillation of the vortex wakes over the slender body. The time-averaged vortex patterns over the slender body are asymmetric, whose orientation is dependent on azimuthal locations of tip perturbations. Therefore, the vortex oscillation is a type of unsteady oscillation around a time-averaged asymmetric vortex structure.

1. Introduction

It has long been known that axisymmetric slender bodies can produce asymmetric vortex wakes at high angles of attack (AOAs), even with zero sideslip.[1–9] The asymmetric vortices can induce large time-averaged side forces which are sometimes even beyond normal forces. Previous research has revealed that the vortex asymmetry primarily arising from imperfections on the nose-tip of a body[3–5] and even natural perturbation from machining tolerance can trigger the development of the asymmetric vortex flow. Since the distribution of machining tolerance is different and random in various models, the experimental results normally show poor reproducibility. If an artificial perturbation, however, is added onto the nose-tip, it can suppress the natural perturbation and dominate the development of the asymmetric vortex flow. By doing this, reproducible time-averaged results can be obtained because the artificial perturbation, its size and position, are pre-determined.[5] The sensitivity of vortex flows over slender bodies to tip imperfections has been exploited for vortex control.[8–10]

The previous experiments[1,6] have revealed that asymmetric vortex wakes over a slender body exhibit a time-averaged multi-vortex structure with an alternate arrangement along a body axis at high AOAs. In the asymmetric vortex system, when a higher vortex breaks away from the body, a new vortex will be yielded under it. As a result, an alternate multi-vortex pattern is formed. However, the flow pattern at the after-body part far away from the fore-body will transit to Karman vortex

* Corresponding author. Tel.: +86 10 82338344.
E-mail address: bf-ma@buaa.edu.cn (B. Ma).

Peer review under responsibility of Editorial Committee of CJA.

Production and hosting by Elsevier

http://dx.doi.org/10.1016/j.cja.2014.06.011

shedding at some locations downstream if the cylinder part is sufficiently long.[6,11–13]

Besides the vortex shedding at an after-body, some intrinsic unsteady features also exist for the vortex system, as summarized in the review paper.[14] The unsteady characteristics of asymmetric vortices were examined in detail by Degani et al.[15–17] They found initially unsteadiness on flow fields over slender bodies using numerical simulation,[15] thus carrying out experiments to identify these unsteady flows.[16] Their experiments revealed three types of unsteady phenomena, including low-frequency Karman vortex shedding, high-frequency shear-layer unsteadiness, and vortex interaction at moderate frequencies. Among these unsteady phenomena, low-frequency vortex shedding has the largest fluctuating amplitude, but can be suppressed by a splitter plate on the leeward side of the body.[17] However, in Degani et al.'s experiments, the pressure transducers for monitoring pressure signals were distributed only on the cylinder part of the slender body, so the unsteadiness for fore-body vortices could not be detected. It is expected that with increasing AOAs, the higher vortex will break away from the body surface earlier and the whole vortex system will move forward in position. Therefore, at sufficiently high AOAs, the time-averaged asymmetric vortices will be retained only at the fore-body part. The experiments by Zilliac et al.[18] using a smoke visualization showed qualitatively that at AOAs of more than 65°, the flow could be divided into three parts: a pair of stationary vortices over a fore-body, oblique shedding over a cylinder part adjacent to the fore-body, and parallel shedding around an inclined cylinder part far downstream. They believed that the vortices near the fore-body were nearly stationary with no significant unsteadiness. Hoang et al.[19] measured the unsteady flow fields around a hemisphere-cylinder body using hotwires and detected a type of unsteady phenomenon where the frequencies of fluctuations are lower than the ones of Karman vortex shedding, but the sources of fluctuations were not clear, and they conjectured that the low frequency fluctuations could be caused by fore-body vortex heaving. Ma et al.[20,21] also studied the difference of unsteadiness at the fore-body and after-body of a slender body at extreme high AOAs. The pressure signals' measured and associated spectra indicated that the unsteadiness was primarily Karman vortex shedding at the after-body, but there exists lower frequency fluctuations at the fore-body. They speculated that the lower-frequency fluctuations come from fore-body vortex fluctuations.

The previous studies mentioned above implied that a type of low-frequency unsteady phenomena seemed to exist around the fore-body of a slender body at high AOAs, frequencies of which are lower than the ones of Karman vortex shedding. However, the previous studies only presented the results based on single-point measurements, so the effects of the unsteady phenomena on the side forces of slender bodies cannot be evaluated. More importantly, the flow sources of these fluctuations need to be confirmed further. In addition, the variation of the unsteady fluctuations with Reynolds numbers is also an interesting issue worth research.

The present study will focus on the vortex unsteadiness around the fore-body of a slender body at sufficiently high AOAs and try to answer the above questions based on multi-points pressure and particle image velocimetry (PIV) measurements.

2. Experimental setup

All experiments were carried out in the D4 Wind Tunnel of Institute of Fluid Mechanics of Beihang University (BUAA). The wind tunnel is a low speed, low noise and closed-return tunnel that can be run with either an open or closed test section. The test sections are 1.5 m wide, 1.5 m high and 2.5 m long, with a turbulence level of less than 0.1%. The open test section was used in the present experiments, and the model layout in the wind tunnel is illustrated in Fig. 1(a). The AOAs of the model are varied through sideslip angles for performing PIV more conveniently. The laser sheet for PIV illuminates the leeward side of the fore-body normal to the body's axis from one side. The PIV snapshots were taken from a front view, but presented in their mirror images in the following "Results" section, equivalently seen from a rear view.

The experimental model is a pointed ogive-tangent cylinder with a fineness ratio of $8D$, including a $3D$ fore-body (D is the diameter of cylinder, and D = 90 mm), as shown in Fig. 1(b). There is a small rotatable nose of 27.5 mm at the front of the fore-body, which is used to change the orientation of tip perturbations. An artificial tip perturbation was added on the nosetip in order to suppress natural imperfections on the tip, ensuring the repeatability of time-averaged flow fields, as shown in Fig. 1(b) (d is the diameter of tip perturbation, d = 0.2 mm). The perturbation is placed on two azimuthal angles of +45° and −45° in experiments.

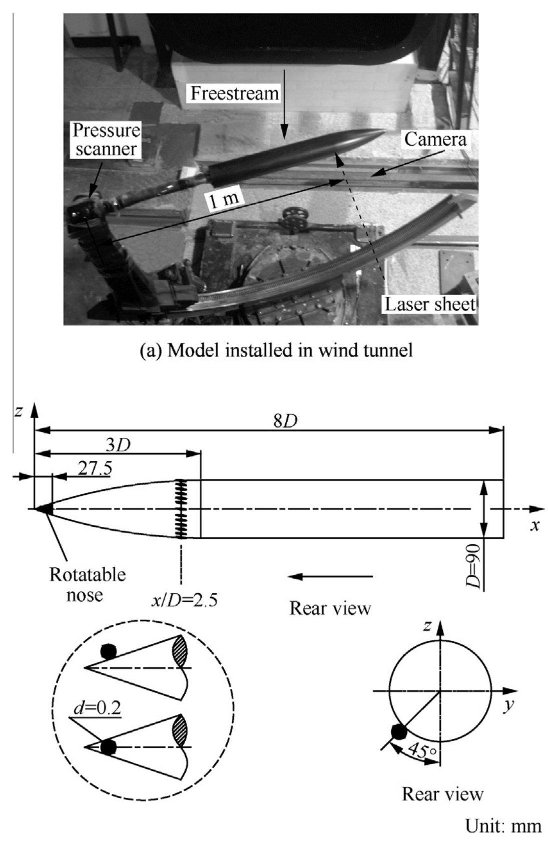

(a) Model installed in wind tunnel

(b) Model and tip perturbation

Fig. 1 Experimental layout and model.